

# Explorations of the Softmax Space: Knowing When the Neural Network Doesn't Know...

Daniel Sikar <sup>\*</sup>, Artur Garcez and Tillman Weyde

Department of Computer Science, School of Science and Technology, City, University of London

**Abstract.** Ensuring the reliability and safety of automated decision-making is crucial. This paper proposes a new approach for measuring the reliability of predictions in machine learning models. We analyze how the outputs of a trained neural network change using clustering to measure distances between outputs and class centroids. We propose this distance as a metric to evaluate the confidence of predictions. We assign each prediction to a cluster with centroid representing the mean softmax output for all correct predictions of a given class. We then define a safety threshold for a class as the smallest distance from an incorrect prediction to the given class centroid. We evaluate the approach on the MNIST and CIFAR-10 datasets using a Convolutional Neural Network and a Vision Transformer, respectively. The results show that our approach is consistent across these data sets and network models, and indicate that the proposed metric can offer an efficient way of determining when automated predictions are acceptable and when they should be deferred to human operators.

## 1 Introduction

Ensuring the reliability and safety of automated decision-making systems is important, particularly in high-impact areas where there exists potential for significant harm from errors [1]. Machine learning (ML) models, while powerful, are susceptible to making erroneous predictions when faced with data that differs from the distribution that they were trained on [22]. This phenomenon, known as distribution shift, poses a significant challenge in deploying ML in real-world scenarios [39].

Distribution shift is a pervasive issue in ML, occurring when the distribution of the data used to train a model differs from the distribution of the data that the model encounters during deployment [39]. This discrepancy can lead to a significant degradation in model performance, as it may struggle to generalize to the new, unseen data [20].

Distribution shifts can manifest itself in various forms, such as covariate shift, concept drift, and domain shift [34]. Covariate shift arises when the input data distribution changes while the conditional distribution of the output given the input remains the same [44]. Concept drift occurs when the relationship between the input and output variables changes over time [13]. Domain shift refers to the situation where the model is trained on data from one domain but applied to data from a different domain [38].

To quantify and address distribution shift, researchers have developed various metrics and techniques. One common approach is to use statistical divergence measures, such as Kullback-Leibler (KL)

divergence [27] or Maximum Mean Discrepancy (MMD) [17], to assess differences in training and test data distributions. These metrics provide a quantitative understanding of the extent of the distribution shift.

Another approach is to employ domain adaptation techniques, which aim to align the feature distributions of the source and target domains [47]. This can be achieved through methods such as importance weighting [45], feature transformation [37], or adversarial learning [14]. These techniques seek to mitigate the impact of distribution shift by making the model more robust to changes in the data distribution.

Recent work has also focused on developing algorithms that can detect and adapt to distribution shift in real-time [31]. These methods often rely on monitoring the model's performance on a stream of data and adjusting the model's parameters or architecture when a significant drop in performance is detected [3]. Such adaptive approaches are particularly relevant in dynamic environments where the data distribution is likely to change over time.

Therefore, distribution shift is a significant challenge that can lead to poor model performance if not addressed properly. As ML models are increasingly deployed in real-world applications, developing robust methods to handle distribution shift remains an important area of research.

In this paper, we propose a novel approach for quantifying the reliability of predictions made by neural networks under distribution shift. Our method leverages clustering techniques to measure the distances between the outputs of a trained neural network and class centroids in the softmax distance space. By analyzing these distances, we develop a metric that provides insight into the confidence that one may attribute to the model's predictions. We adopt the most conservative threshold value at which model predictions are expected to be 100% accurate. The proposed metric offers a computationally efficient, practical way to determine when to accept an automated prediction and when human intervention may be necessary.

Furthermore, we explore the relationship between the distance to class centroids and the model's predictive accuracy. Our findings confirm as expected that classes predicted more accurately by the model tend to have lower softmax distances to their respective centroids. This observation highlights the potential for using the changes observed in the softmax distribution as a proxy for our confidence in the model's predictions. The objective is to establish a closer link than thus far identified by the literature between the distance-based metrics proposed for distribution shift and the approaches that measure the drop in model accuracy. It is expected to offer a better understanding of the connection between model performance and reli-

<sup>\*</sup> Corresponding Author. Email: daniel.sikar@city.ac.uk.

ability, that is, accuracy and how confident we are in the predictions of neural networks.

The main contributions of this paper are:

- A new lightweight approach for quantifying the reliability of neural networks using distance metrics and clustering to take full advantage of the learned softmax distributions. The method requires minimal computational overhead, using only the existing softmax outputs and a set of centroids and thresholds, without additional network modifications or training.
- A combined analysis of the metric-based and accuracy-based methods to tackle distribution shift, with experimental results showing consistency of the proposed approach across CNN and ViT architectures.

## 2 Background

**Softmax prediction probabilities:** The concept of using the entire set of softmax prediction probabilities, rather than solely relying on the maximum output, has been extensively studied in the context of enhancing the safety, robustness, and trustworthiness of machine learning models. By considering the complete distribution of class predictions provided by the softmax output, more reliable and informative prediction pipelines may be developed, that go beyond point estimates [12]. This approach enables the exploration of uncertainty quantification, anomaly detection, and other techniques that contribute to building safer, more robust, and trustworthy autonomous systems.

Uncertainty quantification is a crucial aspect of reliable machine learning systems, as it allows for the estimation of confidence in the model’s predictions [26]. These methods help identify instances where the model is less confident, enabling the system to defer to human judgment or take a more conservative action in safety-critical scenarios [33].

Moreover, the softmax probabilities can be utilized for anomaly detection, which is essential for identifying out-of-distribution (OOD) samples or novel classes that the model has not encountered during training [21]. By monitoring the softmax probabilities, thresholding techniques can be applied to detect anomalies based on the distribution of the predictions [29]. This enables the system to flag potentially problematic inputs and take appropriate actions, such as requesting human intervention or triggering fallback mechanisms.

The use of softmax probabilities also facilitates the development of more robust models that can handle adversarial examples and other types of input perturbations [16]. Adversarial attacks aim to fool the model by crafting input samples that lead to incorrect predictions with high confidence [46]. By considering the entire softmax distribution, defensive techniques such as adversarial training [32] and input transformations [19] can be applied to improve the model’s robustness against these attacks.

Furthermore, the softmax probabilities provide valuable information for interpretability and explainability of the model’s decisions [40]. By analyzing the distribution of the predictions, insights can be gained into the model’s reasoning process and the factors that contribute to its outputs. This transparency is crucial for building trust in the system and facilitating human-machine collaboration [7].

The importance of leveraging the entire softmax distribution extends to various domains, including autonomous vehicles [33], medical diagnosis [28], and financial risk assessment [11]. In these safety-critical applications, the consequences of incorrect predictions can be severe, and relying solely on the maximum softmax output may not

provide sufficient safeguards. By considering the full distribution of predictions, more informed and reliable decisions can be made, reducing the risk of catastrophic failures.

However, the use of softmax probabilities is not without challenges. The calibration of the model’s predictions is an important consideration, as poorly calibrated models may lead to overconfident or underconfident estimates [18]. Techniques such as temperature scaling [18] and isotonic regression [51] can be applied to improve the calibration of the softmax probabilities, ensuring that they accurately reflect the model’s uncertainty.

By considering the complete distribution of class predictions, techniques can be employed to develop more reliable and informative prediction pipelines.

**Clustering:** Clustering algorithms are essential for discovering structures and patterns in data across various domains [23, 50]. K-means, a widely used algorithm, efficiently assigns data points to the nearest centroid and updates centroids iteratively [30]. However, it requires specifying the number of clusters and is sensitive to initial centroid placement [2]. Hierarchical clustering creates a tree-like structure by merging or dividing clusters [25] but may not scale well to large datasets [35]. Density-based algorithms, like DBSCAN, identify clusters as dense regions separated by lower density areas [10, 42].

Other applications include image segmentation for object detection [43], anomaly detection for fraud and intrusion detection [5], customer segmentation for targeted marketing [36], and bioinformatics for gene expression analysis and disease subtype identification [9, 24]. The choice of algorithm depends on data characteristics, desired cluster properties, and computational resources [41].

Given the context and to the best of our knowledge, no prior work exists in using softmax distance to class centroid to put a threshold on the trust in the model’s predictive accuracy in classification tasks.

## 3 Clustering and Softmax Distance as a Confidence Metric

We consider a neural network output vector  $\mathbf{p} = (p_1, p_2, \dots, p_K)$  where  $\sum p_i = 1$ , representing a probability distribution obtained by normalizing the logit vector  $\mathbf{z} = (z_1, z_2, \dots, z_K)$  through the softmax function,  $p_i = \text{softmax}(z_i) = e^{z_i} / \sum_{j=1}^K e^{z_j}$ . For example, given  $\mathbf{p} = [0.01, 0.01, 0.01, 0.01, 0.9, 0.01, 0.01, 0.01, 0.01, 0.01]$ , the predicted class is ‘4’, corresponding to the highest value at index five, reflecting the confidence of the prediction for each class from ‘0’ to ‘9’. The logits, representing log-likelihoods of class memberships, are related to probabilities by  $z_i = \log(p_i / (1 - p_i))$  where  $z_i$  is the logit for class  $i$ , and  $p_i$  is the probability of the input belonging to class  $i$  [15, 4].

We store the predictions for MNIST and CIFAR-10 datasets in a matrix  $\mathbf{M} \in \mathbb{R}^{n \times 12}$ , where  $n$  is the number of predictions, the first ten columns are the softmax probabilities, column 11 is the true class and column 12 is the predicted class.

To obtain cluster centroids  $\mathbf{C} \in \mathbb{R}^{10 \times 10}$  we calculate the mean of all correct predictions from the training datasets with Algorithm 1. To calculate the softmax distance threshold we use all incorrect predictions with Algorithm 2.

**Geometric Characteristics of Probability-Constrained Cluster Spaces:** Cluster centroids produced by softmax layer outputs adhere to valid probability distributions. This requires each coordinate  $c_i$  to satisfy  $0 \leq c_i \leq 1$  and the sum  $\sum_{i=1}^n c_i = 1$ , confining the centroids to the vertices and interior of the standard  $(n - 1)$ -dimensional simplex. For two such centroids  $\mathbf{c}_1$  and  $\mathbf{c}_2$  within the  $n$ -dimensional unit

---

**Algorithm 1** K-Means Centroid Initialisation from Softmax Outputs

---

**Require:** *correct\_preds*: array of shape  $(n, 12)$ , where  $n$  is the number of correct predictions  
**Ensure:** *centroids*: array of shape  $(10, 10)$ , initialised centroids for each digit class

- 1: *probs\_dist*  $\leftarrow$  *corrects\_preds*[:, : 10]  $\triangleright$  Extract probability distribution for each digit
- 2: *centroids*  $\leftarrow$  zeros((10, 10))  $\triangleright$  Initialise centroids array
- 3: **for** *digit*  $\leftarrow$  0 to 9 **do**
- 4: *indices*  $\leftarrow$  where(argmax(*probs\_dist*, axis = 1) == *digit*)[0]  $\triangleright$  Find indices of rows where digit has highest probability
- 5: *centroid*  $\leftarrow$  mean(*probs\_dist*[*indices*], axis = 0)  $\triangleright$  Compute mean probability distribution for selected rows
- 6: *centroids*[*digit*]  $\leftarrow$  *centroid*  $\triangleright$  Assign centroid to corresponding row in centroids array
- 7: **end for**
- 8: **return** *centroids*

---

hypercube under these constraints, the Euclidean distance between centroids  $\mathbf{c}_1, \mathbf{c}_2 \in [0, 1]^n$  is  $d(\mathbf{c}_1, \mathbf{c}_2) = \sqrt{\sum_{i=1}^n (c_{1i} - c_{2i})^2}$ . When enforcing probabilistic constraints via softmax normalization, the maximum achievable distance between centroids remains bounded by  $\sqrt{2}$ , independent of the dimensionality  $n$ .

**Meta-Centroid as a Unified Reference:** To establish a central reference point for analyzing class relationships in probability-constrained cluster spaces, we derive a meta-centroid representative of all class centroids. This meta-centroid serves as a geometric "anchor" within the simplex, enabling consistent comparisons. We evaluate three candidate formulations—arithmetic, weighted, and geometric mean:

- **Arithmetic mean**  $\mathbf{c}_{\text{arith}} = \frac{1}{k} \sum_{i=1}^k \mathbf{c}_i$ , yielding uniform weighting across class centroids.
- **Weighted mean**  $\mathbf{c}_{\text{weighted}} = \sum_{i=1}^k w_i \mathbf{c}_i$ , where weights  $w_i \propto 1/(\text{avg distance of } \mathbf{c}_i \text{ to others})$ , prioritizing centrally located centroids.
- **Geometric mean**  $\mathbf{c}_{\text{geo}} \propto \exp\left(\frac{1}{k} \sum_{i=1}^k \log \mathbf{c}_i\right)$ , enforcing multiplicative "balance" in the probability space.

All three meta-centroids satisfy  $\sum_{j=1}^n c_j = 1$  (verified numerically with the set of correct predictions for the MNIST training dataset). Despite nearly identical average distances to original centroids ( $\approx 0.931$  for arithmetic/weighted vs.  $0.934$  for geometric), the geometric mean was selected for its alignment with the multiplicative structure of softmax probability spaces, even at a marginal cost in representational proximity.

**Convolutional Neural Network:** A Convolutional Neural Network (CNN) is used to classify handwritten digits from the MNIST dataset, consisting of 60,000 training images and 10,000 testing images, each of size 28x28 grayscale (single channel) pixels, representing digits from 0 to 9.

The CNN architecture, implemented using PyTorch, consists of two convolutional layers followed by two fully connected layers. The first convolutional layer has 16 filters with a kernel size of 3x3 and a padding of 1. The second convolutional layer has 32 filters with the same kernel size and padding. Each convolutional layer is followed by a ReLU activation function and a max-pooling layer with a pool size of 2x2. The output of the second convolutional layer is flattened and passed through two fully connected layers with 128 and 10 neurons, respectively. The final output is passed through a log-softmax

function to obtain the predicted class probabilities. The model was

---

**Algorithm 2** Find Minimum Softmax Distances to Centroids for Incorrectly Predicted Digits (Threshold)

---

- 1: **procedure** FINDMINDISTANCES(*data*)
- 2: *labels*  $\leftarrow$  [0, 1, 2, 3, 4, 5, 6, 7, 8, 9]
- 3: *thresh*  $\leftarrow$  empty array of shape (10, 2)
- 4: **for** *i*  $\leftarrow$  0 to 9 **do**
- 5: *label*  $\leftarrow$  *labels*[*i*]
- 6: *min\_dist*  $\leftarrow$  min(*data*[*data*[:, 1] == *label*, 0])
- 7: *thresh*[*i*, 0]  $\leftarrow$  *min\_dist*
- 8: *thresh*[*i*, 1]  $\leftarrow$  *label*
- 9: **end for**
- 10: **return** *thresh*
- 11: **end procedure**

---

trained using the Stochastic Gradient Descent (SGD) optimizer with a learning rate of 0.01 and a batch size of 64. The learning rate was determined using a custom learning rate function that decreases the learning rate over time. The Cross-Entropy Loss function was used as the criterion for optimization. The model was trained for 10 epochs.

The MNIST dataset was preprocessed using a transformation pipeline that converted the images to PyTorch tensors and normalized the pixel values to have a mean of 0.5 and a standard deviation of 0.5. The dataset was then loaded using PyTorch's DataLoader, for batch processing and shuffling of the data.

The total number of parameters for the MNIST classification CNN is 206,922 and took 5m6s to train on a Dell Precision Tower 5810 with a 6-core Intel Xeon Processor and 32GB memory running Ubuntu 18.04.

**Vision Transformer:** The Vision Transformer (ViT) architecture [8] is implemented using the Hugging Face Transformers [48] library. The model used in this study, 'google/vit-base-patch16-224-in21k' [49], is pre-trained on the ImageNet-21k dataset [6], which contains 14 million labeled images. The pre-trained model is then fine-tuned on the CIFAR-10 dataset. The ViT model divides an input image into patches and processes them using a Transformer encoder. The model used in this study has a patch size of 16x16 and an image size of 224x224. The ViT model outputs a representation of the image, which is then passed through a linear layer to obtain the final class probabilities. The model has 86.4M parameters and is fine-tuned to classify images from the CIFAR-10 dataset, consisting of 50,000 training images and 10,000 testing images, each of size 32x32 pixels, representing 10 different classes: airplane, automobile, bird, cat, deer, dog, frog, horse, ship, and truck.

The data preprocessing pipeline involves on-the-fly data augmentation using the torchvision library's transforms module. The training data undergoes random resized cropping, random horizontal flipping, conversion to a tensor, and normalization. The validation and testing data are resized, center-cropped, converted to a tensor, and normalized.

The model is trained using the Hugging Face Trainer API. The learning rate is set to  $2 \times 10^{-5}$ , the per-device train batch size is 10, the per-device eval batch size is 4, and the number of training epochs is 3. The weight decay is set to 0.01. The model is trained on Google Colab Pro, T4 GPU hardware accelerator with high ram.

## 4 Experimental Results and Discussion

In this section, we present and discuss our results for CIFAR-10/ViT and MNIST/CNN. We focus on the MNIST training dataset results

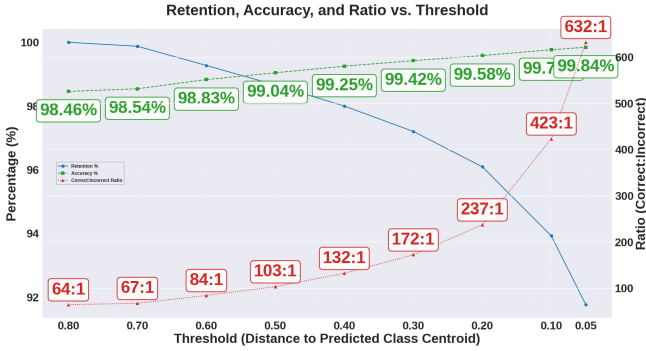


**Figure 1:** Retention, accuracy and correct-incorrect ratio vs Threshold for the CNN on the MNIST dataset.

as they show similar trends as observed in both architectures and training and testing datasets. The confusion matrix shown in Figure 2 provides some insights into what the most likely MNIST misclassifications are. The training dataset contains 60,000 images and is well-balanced (each digit class has approximately 6,000 examples). On the diagonal we see the number of correct classifications and off-diagonal we see the pair-wise incorrect classifications e.g. there are 54 occurrences of 8 misclassified as a 9. We note that number zero is the digit less likely (sum of the row values minus the diagonal is the smallest), and number eight is the digit most likely to be misclassified (sum of the row values minus the diagonal is the greatest). Other digits that are less likely to be misclassified are digits one, six and five. Digit eight is likely to be misclassified as six or nine, while digit three is likely to be misclassified as two, five or nine.

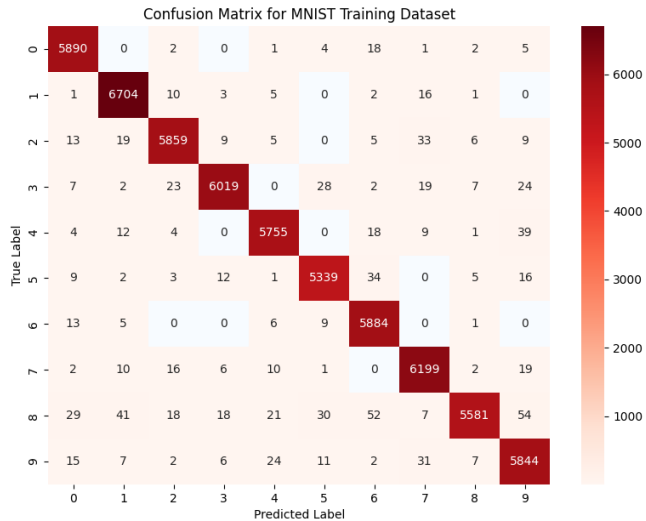


**Figure 2:** Confusion Matrix showing results for the CNN training dataset classification.

The average of all the softmax outputs on the diagonal ( $>59k$  examples) and of all values off diagonal ( $<1k$  examples) are shown in Figure 3. The top row shows the results for the correct predictions, and the bottom row for the incorrect predictions. Looking at the plot on the top left, the average softmax output for all digit 0 predictions, we see on the x axis the class digits, from 0 to 9 and on the y axis, the softmax output on a logarithmic scale. The bar for index 0 is the highest by over two orders of magnitude. We see this pattern repeating for every digit e.g., in the next plot for Digit 1, x axis index 1 bar is the highest, and so on. The average over all correct predictions show low entropy, reflecting the model’s confidence, or certainty in the predictions. On the bottom row are the incorrect predictions. On

the far left are all the examples that were misclassified as digit 0. The bar for index 0 is still the highest, except by only one order of magnitude, and see this pattern repeated for all incorrectly classified digits. In the case of incorrect classifications, the average over all incorrect predictions show high entropy, reflecting the model’s uncertainty in the predictions.

**Clustering:** The average softmax outputs for all correct classifications provide a good starting point for the K-Means algorithm centroids, converging quickly with good separation of clusters. This unsupervised learning method manages to assign all but two of the  $>59k$  correctly classified examples - in the supervised learning task - to the correct class centroids i.e. all digits 0 are assigned to cluster 0. We say the unsupervised (clustering) task presents *high fidelity* in relation to the supervised (classification) learning task, and is a good proxy to assess model confidence in its predictions, the correlation between cluster assignments and true labels providing independent validation. We computed the all pairwise distances between the 10-class centroids ( $\binom{10}{2} = 45$  pairs) in the softmax space. The distances exhibit  $d_{min} = 1.368$ ,  $d_{max} = 1.402$ ,  $\mu = 1.389$  and  $\sigma = 0.009$ . These values approach  $\sqrt{2}$ , the maximum distance between points in the probability-constrained simplex, indicating the model distributes classes at near-maximal separation in the output space. The supervised learning task achieved this separation through gradient descent on the cross-entropy loss; the unsupervised learning task confirms what has been induced by the classification training.

Now we examine one out of the two edge cases where images are correctly classified but incorrectly clustered, to understand the softmax output and distance to class centroid patterns. Figure 4 shows a correctly classified digit six, where the softmax output for digits 5 and 6 is 0.491 and 0.495 respectively and the distance of the prediction to centroids 5 and 6 are 0.696 and 0.697 respectively. Therefore, the softmax output is marginally higher for digit six, while the softmax output is marginally closer to the class 5 centroid. The softmax output pattern shows high entropy, while the distances to class centroids (notice y axis is not on logarithmic scale in this case) shows that digit is about 1.2 units away from all class centroids and close to 0.7 from both centroids 5 and 6. This example illustrates a case where the model exhibits uncertainty between two plausible classes, positioning the output almost equidistant between their centroids in the probability simplex. The slight discordance between classification and clustering in this case reveals a boundary condition in the model’s decision space.

The next example presents a contrasting case to the previous edge case. Figure 5 shows a digit six where the softmax output assigns 0.993 probability to class 6, with all other classes receiving probabilities below 0.004 (y axis is logarithmic). The distance to centroid 6 is 0.00153, while distances to all other centroids are approximately 1.4 units. This represents a typical case where both classification and clustering align with high confidence, positioning the output near the class 6 centroid in the probability simplex. The low entropy in softmax outputs and clear separation in centroid distances indicate unambiguous class membership.

**Softmax Distance to Class Centroid Statistics:** Having analyzed inter-centroid distances and edge cases in the model’s decision space, we now investigate how these geometric properties can be leveraged to ensure the reliability of automated decision-making establish at runtime, when there are no labels. Table 1 quantifies the trade-offs as we vary threshold distances from class centroids. Column **Thresh** shows centroid-to-threshold distance values in descending order, starting at 0.8. Column **Ret %** shows the ratio of correct predictions that are retained, that is, are not being discarded due to a conser-

MNIST Training Data - Softmax Average Distributions for Correct and Incorrect Digit Predictions

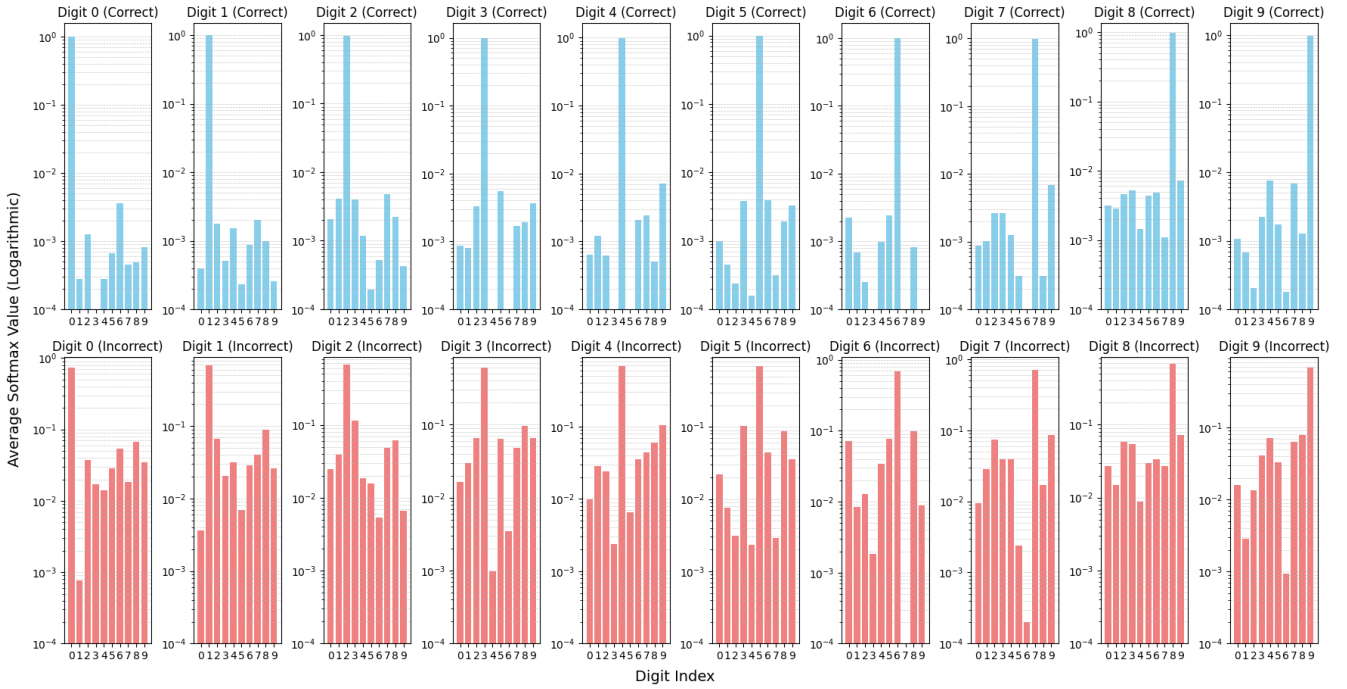


Figure 3: Average Softmax Probabilities for Correctly and Incorrectly Classified Digits in the MNIST Training Dataset.

**Table 1:** Enhanced Threshold Analysis with Meta Metrics. Key columns: **Thresh**: Class threshold; **Ret%**: Retention percentage; **Acc%**: Accuracy percentage; **Corr**: Correct predictions retained; **Incor**: Incorrect predictions retained; **CLost**: Cumulative correct lost; **CElim**: Cumulative incorrect eliminated; **Ratio**: Correct:Incorrect ratio; **MetaT**: Meta threshold; **PtsIn**: Points inside meta hypersphere; **NoCls**: Points outside both class and meta hyperspheres; **%CLst**: Percentage of total correct lost; **%CEm**: Percentage of total incorrect eliminated; **%Pts**: Percentage of dataset inside meta hypersphere; **%NCl**: Percentage of dataset in no-class zone.

Thresh	Ret%	Acc%	Corr	Incor	CLost	CElim	Ratio	MetaT	PtsIn	NoCls	%CLst	%CEm	%Pts	%NCl
0.80	100.00%	98.46%	59073	926	1	0	64:1	0.1337	0	1	0.0017%	0.00%	0.00%	0.0017%
0.70	99.87%	98.54%	59048	876	26	50	67:1	0.2337	0	76	0.0440%	5.40%	0.00%	0.1267%
0.60	99.27%	98.83%	58863	699	211	227	84:1	0.3337	5	433	0.3572%	24.51%	0.01%	0.7217%
0.50	98.66%	99.04%	58626	568	448	358	103:1	0.4337	60	746	0.7584%	38.66%	0.10%	1.2433%
0.40	98.00%	99.25%	58355	442	719	484	132:1	0.5337	274	929	1.2171%	52.27%	0.46%	1.5483%
0.30	97.20%	99.42%	57981	338	1093	588	172:1	0.6337	889	792	1.8502%	63.50%	1.48%	1.3200%
0.20	96.09%	99.58%	57411	242	1663	684	237:1	0.7337	1830	517	2.8151%	73.87%	3.05%	0.8617%
0.10	93.92%	99.76%	56219	133	2855	793	423:1	0.8337	3214	434	4.8329%	85.64%	5.36%	0.7233%
0.05	91.76%	99.84%	54969	87	4105	839	632:1	0.8837	4904	40	6.9489%	90.60%	8.17%	0.0667%

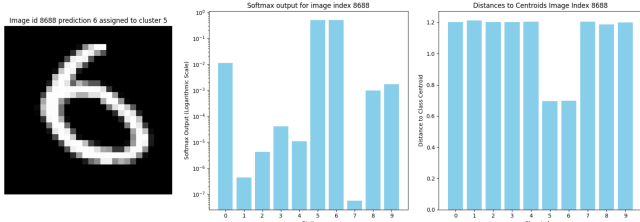


Figure 4: Left to right, MNIST Training Data Image ID 8688 digit 6, the network softmax output and the distances to class centroids, correctly classified as 6 and incorrectly clustered as 5.

vation threshold setting. At 0.8 threshold, the retention is 100%, that is, no "good" predictions have been lost. Column **Acc%** shows the accuracy of the model at the given threshold. Column **Corr** shows the number of correct prediction at the given threhsold, that is the sum of all cases where the softmax output is nearer to the class centroid than the threshold. Reminding ourself that we are looking at results for the MNIST training dataset, in our 10-dimensional cluster-space.

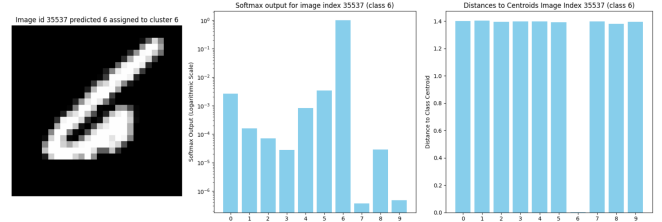


Figure 5: Left to right, MNIST Training Data Image ID 35537 digit 6, the network softmax output and the distances to class centroids, correctly classified and correctly clustered as 6.

**Incor** is the number of incorrect predictions below threshold. It is important to note that all incorrect classifications are at a distance of less than 0.8 to class centroids. **CLost** is the cumulative summ of correct predictions "lost" because the are above the threshold. At 0.8 one correct prediction is lost because it is above the threshold. **CElim** has the number of incorrect predictions that have been "eliminated" due to the threshold. We see that at 0.8, none were eliminated. **Ratio**

is the ratio of correct:incorrect predictions below the threshold, so at 0.8, there are 64 correct for every incorrect prediction. **MetaT** is the difference between the geometric mean distance (0.93 approx) to the meta-centroid, discussed in section 3 and the threshold. Note this quantity is a radius that defines the volume of the meta hypersphere, when the majority of examples the network "knows it doesn't know" will end up. **PtsIn** are the number of points inside the meta hypersphere. **NoCls** are the points that are neither in the class clusters/hyperspheres nor in the meta hypersphere. These could be in interstitial regions between hyperspheres or elsewhere. Note the sum of **CLost** and **CElim** is equal to the sum of **PtsIn** and **NoCls**. **%CLst** is the percentage of **CLost** divided by **Corr** plus **CLost**, **%CEm** is the percentage of **CElim** divided by **Incor** plus **CElim**. **%Pts** is the number of points **PtsIn** inside the meta hypersphere by the total number of examples (60,000) as a percentage. **%NCI** is the number of **NoCI** by the total number of examples as a percentage.

**Enhanced Threshold Analysis:** The ratio of correct to incorrect predictions **Ratio** shows exponential increase as the threshold becomes more selective, rising from 64:1 at the largest threshold (0.80) to 632:1 at the smallest threshold (0.05). The cumulative number of correct predictions lost **CLost** increases as the threshold decreases, the rate of loss accelerates in the lower threshold ranges. The cumulative elimination **CElim** of incorrect predictions increases from 0 to 839 as the threshold decreases. The elimination rate is highest in the upper threshold ranges and shows diminishing returns below 0.20, ultimately removing 90.60% of incorrect predictions at the lowest threshold. The number of points inside the meta-hypersphere **PtsIn** increases from 0 to 4,904 as the threshold decreases. The growth begins slowly with 5 points at 0.60, accelerates through the middle ranges, and reaches 8.17% of the dataset at the lowest threshold. This represents a growing zone of abstention (the model/pipeline abstaining from making predictions) as the meta-threshold expands. The no-class points **NoCls** exhibit a non-monotonic pattern, increasing from 1 to 929 points as the threshold decreases to 0.40, then declining to 40 points at the lowest threshold. This peak of 1.55% of the dataset at threshold 0.40 represents the maximum region where points fall outside both classification and abstention zones, before the meta-threshold extends to lower thresholds. The concentration of these points between thresholds 0.60 and 0.20, mirroring the **CElim** trend suggests this range contained the majority of misclassifications.

This can also be verified by **%NCI**. The accuracy (**Acc%**) shows consistent improvement as the threshold decreases, rising from 98.46% at threshold 0.80 to 99.84% at 0.05, demonstrating the model's enhanced precision in classification decisions. This improvement in accuracy corresponds with the exponential increase in the correct:incorrect ratio from 64:1 to 632:1, indicating increasingly confident predictions. However, this gain comes at a substantial cost in terms of coverage: the retention rate (**Ret%**) drops from 100% to 91.76%, with the model losing 4,104 correct predictions (6.95% of total correct predictions, as shown by **%CLst**). This represents a trade-off between prediction confidence and dataset coverage, where a 1.38 percentage point improvement in accuracy is achieved at the cost of excluding approximately 7% of correct predictions. The inflection point in this trade-off appears around threshold 0.30, where the accuracy gain rate begins to plateau while the retention loss continues to accelerate.

Figure 1 shows the inverse relationship between retention and prediction quality metrics. As the distance threshold decreases from 0.80 to 0.05, accuracy improves gradually (98.46% to 99.84%) while the correct:incorrect ratio increases exponentially (64:1 to 632:1). However, retention drops significantly (100% to 91.76%), particularly ac-

celerating below threshold 0.30. This suggests an optimal operating point around 0.30-0.40, where retention remains above 97% while achieving substantial improvements in accuracy (99.25-99.42%) and correct:incorrect ratio (132:1-172:1). Points beyond this threshold could be designated as abstentions or routed to specialized pipelines, balancing the trade-off between prediction confidence and dataset coverage.

## 5 Conclusions and Future Work

We presented a simple approach for quantifying the reliability of neural networks, validating it across distinct network architectures and datasets, with results presented for a representative scenario. Future work will extend this approach to autonomous systems, using simulators for OOD detection.

## References

- [1] D. Amodei, C. Olah, J. Steinhardt, P. Christiano, J. Schulman, and D. Mané. Concrete problems in ai safety. *arXiv preprint arXiv:1606.06565*, 2016.
- [2] D. Arthur and S. Vassilvitskii. k-means++: The advantages of careful seeding. In *Proceedings of the eighteenth annual ACM-SIAM symposium on Discrete algorithms*, pages 1027–1035, 2007.
- [3] M. Baena-García, J. del Campo-Ávila, R. Fidalgo, A. Bifet, R. Gavaldà, and R. Morales-Bueno. Early drift detection method. In *Fourth International Workshop on Knowledge Discovery from Data Streams*, volume 6, pages 77–86, 2006.
- [4] C. M. Bishop. Pattern recognition and machine learning. *Springer*, 2: 645–678, 2006.
- [5] V. Chandola, A. Banerjee, and V. Kumar. Anomaly detection: A survey. *ACM computing surveys (CSUR)*, 41(3):1–58, 2009.
- [6] J. Deng, W. Dong, R. Socher, L.-J. Li, K. Li, and L. Fei-Fei. Imagenet: A large-scale hierarchical image database. In *2009 IEEE conference on computer vision and pattern recognition*, pages 248–255. Ieee, 2009.
- [7] F. Doshi-Velez and B. Kim. Towards a rigorous science of interpretable machine learning. *arXiv preprint arXiv:1702.08608*, 2017.
- [8] A. Dosovitskiy, L. Beyer, A. Kolesnikov, D. Weissenborn, X. Zhai, T. Unterthiner, M. Dehghani, M. Minderer, G. Heigold, S. Gelly, et al. An image is worth 16x16 words: Transformers for image recognition at scale. *arXiv preprint arXiv:2010.11929*, 2020.
- [9] M. B. Eisen, P. T. Spellman, P. O. Brown, and D. Botstein. Cluster analysis and display of genome-wide expression patterns. *Proceedings of the National Academy of Sciences*, 95(25):14863–14868, 1998.
- [10] M. Ester, H.-P. Kriegel, J. Sander, and X. Xu. A density-based algorithm for discovering clusters in large spatial databases with noise. In *Kdd*, volume 96, pages 226–231, 1996.
- [11] G. Feng, J. He, and N. G. Polson. Deep learning-based quantitative trading strategies for stock markets. *arXiv preprint arXiv:1805.01039*, 2018.
- [12] Y. Gal and Z. Ghahramani. Dropout as a bayesian approximation: Representing model uncertainty in deep learning. *International Conference on Machine Learning*, pages 1050–1059, 2016.
- [13] J. Gama, I. Žliobaitė, A. Bifet, M. Pechenizkiy, and A. Bouchachia. A survey on concept drift adaptation. *ACM Computing Surveys (CSUR)*, 46(4):1–37, 2014.
- [14] Y. Ganin, E. Ustinova, H. Ajakan, P. Germain, H. Larochelle, F. Laviolette, M. Marchand, and V. Lempitsky. Domain-adversarial training of neural networks. *The Journal of Machine Learning Research*, 17(1): 2096–2030, 2016.
- [15] I. Goodfellow, Y. Bengio, and A. Courville. *Deep learning*. MIT press, 2016.
- [16] I. J. Goodfellow, J. Shlens, and C. Szegedy. Explaining and harnessing adversarial examples. In *International Conference on Learning Representations*, 2014.
- [17] A. Gretton, K. M. Borgwardt, M. J. Rasch, B. Schölkopf, and A. Smola. A kernel two-sample test. *The Journal of Machine Learning Research*, 13(1):723–773, 2012.
- [18] C. Guo, G. Pleiss, Y. Sun, and K. Q. Weinberger. On calibration of modern neural networks. In *International Conference on Machine Learning*, pages 1321–1330. PMLR, 2017.

- [19] C. Guo, M. Rana, M. Cisse, and L. Van Der Maaten. Countering adversarial images using input transformations. In *International Conference on Learning Representations*, 2018.
- [20] D. Hendrycks and T. Dietterich. Benchmarking neural network robustness to common corruptions and perturbations. *arXiv preprint arXiv:1903.12261*, 2019.
- [21] D. Hendrycks and K. Gimpel. A baseline for detecting misclassified and out-of-distribution examples in neural networks. In *International Conference on Learning Representations*, 2017.
- [22] D. Hendrycks, S. Basart, N. Mu, S. Kadavath, F. Wang, E. Dorundo, R. Desai, T. Zhu, S. Parajuli, M. Guo, et al. The many faces of robustness: A critical analysis of out-of-distribution generalization. In *Proceedings of the IEEE/CVF international conference on computer vision*, pages 8340–8349, 2021.
- [23] A. K. Jain. Data clustering: 50 years beyond k-means. *Pattern recognition letters*, 31(8):651–666, 2010.
- [24] D. Jiang, C. Tang, and A. Zhang. Cluster analysis for gene expression data: A survey. *IEEE Transactions on knowledge and data engineering*, 16(11):1370–1386, 2004.
- [25] S. C. Johnson. Hierarchical clustering schemes. *Psychometrika*, 32(3):241–254, 1967.
- [26] A. Kendall and Y. Gal. What uncertainties do we need in bayesian deep learning for computer vision? *Advances in Neural Information Processing Systems*, 30, 2017.
- [27] S. Kullback and R. A. Leibler. On information and sufficiency. *The Annals of Mathematical Statistics*, 22(1):79–86, 1951.
- [28] C. Leibig, V. Allken, M. S. Ayhan, P. Berens, and S. Wahl. Leveraging uncertainty information from deep neural networks for disease detection. *Scientific Reports*, 7(1):1–14, 2017.
- [29] S. Liang, Y. Li, and R. Srikant. Enhancing the reliability of out-of-distribution image detection in neural networks. In *International Conference on Learning Representations*, 2018.
- [30] S. Lloyd. Least squares quantization in pcm. *IEEE transactions on information theory*, 28(2):129–137, 1982.
- [31] J. Lu, A. Liu, F. Dong, F. Gu, J. Gama, and G. Zhang. Learning under concept drift: A review. *IEEE Transactions on Knowledge and Data Engineering*, 31(12):2346–2363, 2018.
- [32] A. Madry, A. Makelov, L. Schmidt, D. Tsipras, and A. Vladu. Towards deep learning models resistant to adversarial attacks. In *International Conference on Learning Representations*, 2017.
- [33] R. Michelmore, M. Kwiatkowska, and Y. Gal. Evaluating uncertainty quantification in end-to-end autonomous driving control. *arXiv preprint arXiv:1811.06817*, 2018.
- [34] J. G. Moreno-Torres, T. Raeder, R. Alaiz-Rodríguez, N. V. Chawla, and F. Herrera. A unifying view on dataset shift in classification. *Pattern Recognition*, 45(1):521–530, 2012.
- [35] D. Müllner. Modern hierarchical, agglomerative clustering algorithms. *arXiv preprint arXiv:1109.2378*, 2011.
- [36] E. W. Ngai, L. Xiu, and D. C. Chau. Application of data mining techniques in customer relationship management: A literature review and classification. *Expert systems with applications*, 36(2):2592–2602, 2009.
- [37] S. J. Pan and Q. Yang. A survey on transfer learning. *IEEE Transactions on Knowledge and Data Engineering*, 22(10):1345–1359, 2009.
- [38] V. M. Patel, R. Gopalan, R. Li, and R. Chellappa. Visual domain adaptation: A survey of recent advances. *IEEE Signal Processing Magazine*, 32(3):53–69, 2015.
- [39] J. Quiñero-Candela, M. Sugiyama, A. Schwaighofer, and N. D. Lawrence. Dataset shift in machine learning. *The MIT Press*, 2009.
- [40] M. T. Ribeiro, S. Singh, and C. Guestrin. "why should i trust you?" explaining the predictions of any classifier. In *Proceedings of the 22nd ACM SIGKDD International Conference on Knowledge Discovery and Data Mining*, pages 1135–1144, 2016.
- [41] M. Z. Rodriguez, C. H. Comin, D. Casanova, O. M. Bruno, D. R. Amancio, L. d. F. Costa, and F. A. Rodrigues. Clustering algorithms: A comparative approach. *PloS one*, 14(1):e0210236, 2019.
- [42] E. Schubert, J. Sander, M. Ester, H. P. Kriegel, and X. Xu. Dbscan revisited, revisited: why and how you should (still) use dbscan. *ACM Transactions on Database Systems (TODS)*, 42(3):1–21, 2017.
- [43] J. Shi and J. Malik. Normalized cuts and image segmentation. *IEEE Transactions on pattern analysis and machine intelligence*, 22(8):888–905, 2000.
- [44] H. Shimodaira. Improving predictive inference under covariate shift by weighting the log-likelihood function. *Journal of Statistical Planning and Inference*, 90(2):227–244, 2000.
- [45] M. Sugiyama, M. Krauledat, and K.-R. Müller. Covariate shift adaptation by importance weighted cross validation. *The Journal of Machine Learning Research*, 8:985–1005, 2007.
- [46] C. Szegedy, W. Zaremba, I. Sutskever, J. Bruna, D. Erhan, I. Goodfellow, and R. Fergus. Intriguing properties of neural networks. In *International Conference on Learning Representations*, 2013.
- [47] M. Wang and W. Deng. Deep visual domain adaptation: A survey. *Neurocomputing*, 312:135–153, 2018.
- [48] T. Wolf, L. Debut, V. Sanh, J. Chaumond, C. Delangue, A. Moi, P. Cistac, T. Rault, R. Louf, M. Funtowicz, J. Davison, S. Shleifer, P. von Platen, C. Ma, Y. Jernite, J. Plu, C. Xu, T. L. Scao, S. Gugger, M. Drame, Q. Lhoest, and A. M. Rush. Huggingface’s transformers: State-of-the-art natural language processing, 2020.
- [49] B. Wu, C. Xu, X. Dai, A. Wan, P. Zhang, Z. Yan, M. Tomizuka, J. Gonzalez, K. Keutzer, and P. Vajda. Visual transformers: Token-based image representation and processing for computer vision, 2020.
- [50] D. Xu and Y. Tian. A comprehensive survey of clustering algorithms. *Annals of Data Science*, 2(2):165–193, 2015.
- [51] B. Zadrozny and C. Elkan. Transforming classifier scores into accurate multiclass probability estimates. In *Proceedings of the eighth ACM SIGKDD International Conference on Knowledge Discovery and Data Mining*, pages 694–699, 2002.